International Journal of Mechanical Sciences 53 (2011) 436–445

Contents lists available at ScienceDirect

International Journal of Mechanical Sciences

journal homepage: www.elsevier.com/locate/ijmecsci

Vibrations of rectangular plates with internal cracks or slits

C.S. Huang [a,*], A.W. Leissa [b], C.W. Chan [a]

[a] Department of Civil Engineering, National Chiao Tung University, 1001 Ta-Hsueh Rd., Hsinchu 30050, Taiwan
[b] Department of Mechanical Engineering, Colorado State University, Fort Collins, CO 80523, USA

ARTICLE INFO

Article history:
Received 16 January 2009
Received in revised form
27 July 2010
Accepted 29 March 2011
Available online 6 April 2011

Keywords:
Ritz method
Cracked plates
Vibrations
Special admissible functions

ABSTRACT

This work applies the famous Ritz method to analyze the free vibrations of rectangular plates with internal cracks or slits. To retain the important and useful feature of the Ritz method providing the upper bounds on exact natural frequencies, the paper proposes a new set of admissible functions that are able to properly describe the stress singularity behaviors near the tips of the crack and meet the discontinuous behaviors of the exact solutions across the crack. The validity of the proposed set of functions is confirmed through comprehensive convergence studies on the frequencies of simply supported square plates with horizontal center cracks having different lengths. The convergent frequencies show excellent agreement with published accurate results obtained by an integration equation technique, and are more accurate than those obtained by a previously published approach using the Ritz method combined with a domain decomposition technique. Finally, the present solution is employed to obtain accurate natural frequencies and mode shapes for simply supported and completely free square plates with internal cracks having various locations, lengths, and angular orientations. Most of the configurations considered here have not been analyzed in the previously published literature. The present results are novel, and are the first published vibration data for completely free rectangular plates with internal cracks and for plates with internal cracks, which are not parallel to the boundaries.

1. Introduction

Since the Ritz method [1] was proposed in 1908, it has become a popular method on analyzing vibrations of plates because of its high efficiency in yielding accurate solutions. There are hundreds of published papers applying the Ritz method to determine natural frequencies of plates with various shapes and boundary conditions in the monograph of Leissa [2] and review papers [3–5]. However, there are very few works devoted to problems of plates with internal cracks, which can be due to the difficulties on developing good admissible functions for such problems. It is well-known that the success of the Ritz method in accurately solving vibration problems mainly depends on using appropriate admissible functions. Appropriate admissible functions for plates with internal cracks should not only properly describe the stress singularity behaviors at the neighborhood of the crack tips, but also meet the discontinuities of displacement and slopes across cracks.

Only three papers in the published literature employed the Ritz method to analyze vibrations of rectangular plates with internal cracks in literature. Yuan and Dickinson [6] and Liew et al. [7] decomposed the domain under consideration into several sub-domains and used orthogonal polynomials as admissible functions for each sub-domain. They utilized different approaches to enforce the continuities of displacement and slope along the interconnecting boundaries among the sub-domains. Yuan and Dickinson introduced artificial springs along the interconnecting boundaries, while Liew et al. imposed the continuity conditions in an integration sense, but not everywhere along the interconnecting boundaries. Consequently, these two approaches loose an important feature of the Ritz method. Because the constraint conditions across the sub-domain boundaries are not strictly enforced, upper bounds on exact natural frequencies, monotonously converging to exact solutions as the number of admissible functions increases, cannot be guaranteed. Khadem and Rezaee [8] proposed modified comparison functions constructed from Levy's form of solution as the admissible functions to analyze a simply supported rectangular plate with a crack parallel to one side of the plate. Due to Levy's form of solution used in constructing admissible functions, the solutions of Khadem and Rezaee are not suitable for plates with other shapes or boundary conditions. Furthermore, these solutions do not show the stress singularities at the crack tips, so that the solutions cannot be applied to investigate the local behaviors of vibrating plates in the neighborhood of the crack tip.

Several integration equation approaches were proposed to investigate vibrations of cracked rectangular thin plates with

* Corresponding author.
E-mail addresses: cshuang@mail.nctu.edu.tw (C.S. Huang), awleissa@mindspring.com (A.W. Leissa).

0020-7403/$ - see front matter © 2011 Elsevier Ltd. All rights reserved.
doi:10.1016/j.ijmecsci.2011.03.006

simply supported conditions at all edges or two opposite edges and having cracks parallel to one of the edges. Lynn and Kumbasar [9] first studied the vibrations of cracked rectangular plates using a Green's function approach to obtain Fredholm integral equations of the first kind that were numerically solved, while Stahl and Keer [10] and Aggarwala and Ariel [11] formulated the problems under consideration as dual equations that were further reduced to homogeneous Fredholm integral equations of the second kind. Neku [12] employed Levy's form of solution to establish the needed Green's functions in Lynn and Kumbasar's approach [9]. Solecki [13] developed his solution using Navier's form of solution, along with finite Fourier transformations of discontinuous functions for the displacement and slope across the crack. The solutions of Hirano and Okazaki [14] were developed by utilizing Levy's solution and fitting the mixed boundary conditions on the line of the crack by means of a weighted residual method. These approaches are not valid for cracked plates with shapes other than rectangular, or boundary conditions other than simple support.

Although finite element techniques have advantages in easily fitting complex geometry and boundary conditions, few papers were devoted to analyzing vibrations of cracked thin plates based on the classical plate theory because difficultly constructed C^1 type elements are needed. Qian et al. [15] proposed a finite element approach where the stiffness matrix of the element with crack was derived by integrating the stress intensity factor of a finite cracked plate under bending, twisting, and shearing. Krawczuk [16] proposed a solution similar to that of Qian et al. [15], except that the stiffness matrix of the element with crack was expressed in a closed form. Su et al. [17] presented the fractal two-level finite element method combining fractal transformation technique and conventional finite element formulation to model the singular region around a crack tip and regular region of a plate.

Notably, instead of the classical plate theory, the first order shear deformation plate theory, which only requires C^0 type elements, is often applied in finite element formulation for thin plate problems (i.e., in commercial finite element packages). When using such formulation to solve a very thin plate problem, one may face the shear locking problem. Ma and Huang [18] simply used the commercial finite element computer program ABAQUS and selected eight-node two-dimensional shell elements (S8R5) to find natural frequencies of cantilevered thin plates with horizontal or vertical side cracks to verify the correctness of their experimental results. In the last two decades, various extended finite element methods have been proposed to solve for crack problems. Bachene et al. [19] claimed that they were the first ones to present an extended finite element solution for vibrations of cracked plates. Again, they used the first order shear deformation plate theory.

The main purpose of this work is to present a systematic approach to establish proper admissible functions for the Ritz method in analyzing vibrations of thin plates with internal cracks based on the classical plate theory. The proposed admissible functions, which are modified from the corner functions developed by Williams [20] for a sectorial plate, are capable of describing the singular behaviors of stress resultants around the crack tips, and show the discontinuities of transverse displacement and slope across the crack. The validity of the proposed admissible functions is confirmed through comprehensive convergence studies on the frequencies of simply supported square plates with horizontal center cracks having different lengths and comparisons with existing results. Then, the present approach is used to investigate the vibration behavior of simply supported and completely free square plates with internal cracks at different locations, and having different lengths and angular orientations. Numerical results are presented for the frequencies and nodal patterns, few of which have been seen in the previous literature. These results are the most comprehensive and accurate sets of frequencies to date for rectangular plates with internal cracks or slits. They are also the first published vibration data for cracks, which are inclined ($\alpha \neq 0^\circ$) and for completely free plates with internal cracks.

2. Methodology

Fig. 1 shows the geometry of a thin rectangular plate with an internal through crack of length d, having arbitrary location and angular orientation. The well-known Ritz method is applied to determine the natural frequencies of the plate based on the classical plate theory. In the Ritz method, the maximum strain energy ($V_{\max}$) and the maximum kinetic energy ($T_{\max}$) for a plate vibrating harmonically with amplitude $W(x,y)$ and circular frequency ω are (Leissa [2])

$$V_{\max} = \frac{D}{2}\iint_A (W_{,xx}+W_{,yy})^2 - 2(1-\upsilon)(W_{,xx}W_{,yy}-(W_{,xy})^2)dA, \tag{1a}$$

$$T_{\max} = \frac{\omega^2 \rho h}{2}\iint_A W^2 dA, \tag{1b}$$

where D, υ, h, and ρ are the flexural rigidity of the plate, Poisson's ratio, plate thickness, and mass per unit volume, respectively; and the subscript comma denotes partial differentiation with respect to the coordinate defined by the variable after the comma. The vibration frequencies of the plate are obtained by minimizing the energy functional

$$\Pi = V_{\max} - T_{\max}. \tag{2}$$

The admissible functions for representing W in Eq. (1) must satisfy the geometric (i.e. essential) boundary conditions of the problem under consideration. For a rectangular plate with an internal crack, the admissible functions for the transverse displacement are assumed here as the sum of two sets of functions:

$$W = W_p + W_c, \tag{3}$$

where W_p is a set of algebraic polynomials, which forms a mathematically complete set of functions if an infinite number of terms are used; W_c is used to supplement W_p by appropriately describing the important behavior along the crack.

Orthogonal polynomials are used for W_p, and W_p is expressed as

$$W_p(x,y) = \sum_{i=1,2}^{I}\sum_{j=1,2}^{J} A_{ij}P_i(x)Q_j(y), \tag{4}$$

where $P_i(x)$ and $Q_j(y)$ are sets of orthogonal polynomials in x and y directions of the rectangular plate under consideration (see Fig. 1), respectively. These orthogonal polynomials are generated by using a

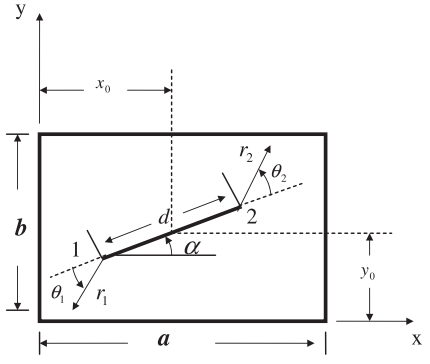

Fig. 1. Dimensions and coordinates for a rectangular plate with an internal crack (x_0 and y_0 locate the center of the crack).

Gram–Schmidt process [21] and satisfy the geometrical boundary conditions of the rectangular plate. Notably, using orthogonal polynomials results in less ill-conditioning of the matrix than using regular polynomials.

The exact solution for a plate with an internal crack has certain special features: singularities of moments and shear forces at the crack tips, and discontinuities of the defection and slope across the crack. These characteristics are not found in $W_p(x,y)$ given in Eq. (4). Consequently, the admissible functions for W_c in Eq. (3) are chosen so as to have them. This work proposes the following set of admissible functions for W_c, which will be termed the modified corner functions,

$$W_c = x^l(a-x)^m y^p (b-y)^q \left\{ \sum_{n=1}^{N_1} C_n \tilde{w}_{n,S}(\lambda_n, r_1, \theta_1, r_2, \theta_2) + \sum_{n=1}^{N_2} D_n \tilde{w}_{n,A}(\lambda_n, r_1, \theta_1, r_2, \theta_2) + \sum_{n=1}^{N_3} E_n \tilde{w}_{n,S}(\lambda_n, r_2, \theta_2, r_1, \theta_1) + \sum_{n=1}^{N_4} F_n \tilde{w}_{n,A}(\lambda_n, r_2, \theta_2, r_1, \theta_1) \right\}, \quad (5)$$

where l, m, p, and q are integers making W_c satisfy the geometric boundary conditions along $x=0$, $x=a$, $y=0$, and $y=b$; $\lambda_n = n/2$, $n=1, 2, \ldots$. When λ_n is an integer, the functions $\tilde{w}_{n,A}$ and $\tilde{w}_{n,S}$ are defined as follows:

$$\tilde{w}_{n,s}(\lambda_n, r_i, \theta_i, r_j, \theta_j) = r_j^{\overline{\kappa}} \hat{w}_{n,S}(\lambda_n, r_i, \theta_i), \quad (6a)$$

$$\tilde{w}_{n,A}(\lambda_n, r_i, \theta_i, r_j, \theta_j) = r_j^{\overline{\kappa}} \hat{w}_{n,A}(\lambda_n, r_i, \theta_i), \quad (6b)$$

where

$$\hat{w}_{n,S}(\lambda_n, r_i, \theta_i) = r_i^{\lambda_n+1} \left(-\frac{\gamma_2}{\gamma_1} \cos(\lambda_n+1)\theta_i + \cos(\lambda_n-1)\theta_i \right), \quad (6c)$$

$$\hat{w}_{n,A}(\lambda_n, r_i, \theta_i) = r_i^{\lambda_n+1} \left(\frac{\gamma_3}{\gamma_1} \sin(\lambda_n+1)\theta_i + \sin(\lambda_n-1)\theta_i \right), \quad (6d)$$

and $\gamma_1 = (\lambda_n+1)(\upsilon-1)$, $\gamma_2 = -\lambda_n(1-\upsilon)+(3+\upsilon)$, $\gamma_3 = \lambda_n(1-\upsilon)+(3+\upsilon)$.

When λ_n is not an integer, the functions $\tilde{w}_{n,A}$ and $\tilde{w}_{n,S}$ are defined as follows:

$$\tilde{w}_{n,s}(\lambda_n, r_i, \theta_i, r_j, \theta_j) = \sin^2(\theta_j/2) r_j^{\kappa} \hat{w}_{n,S}(\lambda_n, r_i, \theta_i), \quad (6e)$$

$$\tilde{w}_{n,A}(\lambda_n, r_i, \theta_i, r_j, \theta_j) = \sin^2(\theta_j/2) r_j^{\kappa} \hat{w}_{n,A}(\lambda_n, r_i, \theta_i), \quad (6f)$$

where

$$\hat{w}_{n,S}(\lambda_n, r_i, \theta_i) = r_i^{\lambda_n+1} \left(\frac{\gamma_3}{\gamma_1} \cos(\lambda_n+1)\theta_i + \cos(\lambda_n-1)\theta_i \right), \quad (6g)$$

$$\hat{w}_{n,A}(\lambda_n, r_i, \theta_i) = r_i^{\lambda_n+1} \left(-\frac{\gamma_2}{\gamma_1} \sin(\lambda_n+1)\theta_i + \sin(\lambda_n-1)\theta_i \right). \quad (6h)$$

The functions $\hat{w}_{n,A}(\lambda_n, r_i, \theta_i)$ and $\hat{w}_{n,S}(\lambda_n, r_i, \theta_i)$ in Eq. (6) are the well-known original corner functions developed according to Williams' solutions [20]. These original corner functions satisfy the static governing equation for a thin plate without loading and the free boundary conditions along the crack, and appropriately describe the stress singularity behaviors at crack tip i (see Fig. 1). The subscripts A and S denote anti-symmetric and symmetric functions with respect to $\theta_i=0$, respectively. The coordinates (r_1,θ_1) and (r_2,θ_2), whose origins are at the two tips of an internal crack, respectively, are shown in Fig. 1.

When λ_n is an integer, $\hat{w}_{n,S}(\lambda_n, r_i, \theta_i)$ and $\hat{w}_{n,A}(\lambda_n, r_i, \theta_i)$ in Eqs. (6c) and (6d) could be linearly dependent with the polynomial admissible functions. Hence, $r_j^{\overline{\kappa}}$ with $\overline{\kappa}$ not equal to an integer, is multiplied to $\hat{w}_{n,S}$ and $\hat{w}_{n,A}$ in order to avoid the possible linear dependence among the admissible functions in W_p and W_c. When $\overline{\kappa}$ is set equal to 1.5, the resulting $\tilde{w}_{n,s}(\lambda_n, r_i, \theta_i, r_j, \theta_j)$ and $\tilde{w}_{n,A}(\lambda_n, r_i, \theta_i, r_j, \theta_j)$ in Eqs. (6a) and (6b), respectively, also match the stress singularity orders at $r_j=0$. Notably, using $\overline{\kappa} < 1.5$ results in incorrect singularity orders for stress resultants at the crack tips, and is not used.

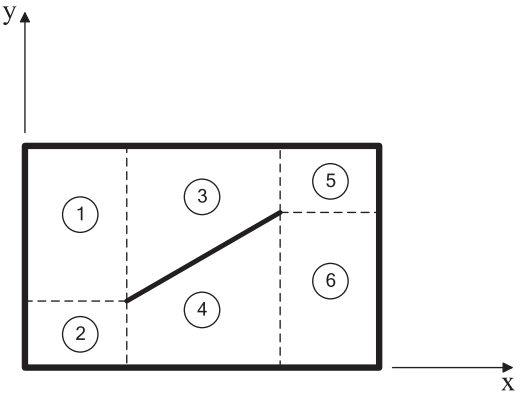

Fig. 2. Six sub-domains for integration.

When λ_n is not an integer, $\hat{w}_{n,A}(\lambda_n, r_i, \theta_i)$ in Eqs. (6h) is not continuous across $\theta_i = \pm\pi$ while the first derivative of $\hat{w}_{n,S}(\lambda_n, r_i, \theta_i)$ in Eq. (6g) with respect to x or y is not continuous across $\theta_i = \pm\pi$. These functions can be used to describe the discontinuity behaviors of the exact solution across the internal crack. However, $\hat{w}_{n,A}(\lambda_n, r_i, \theta_i)$ and $\hat{w}_{n,S}(\lambda_n, r_i, \theta_i)$ also cause the discontinuity behaviors of solutions along the segments with $\theta_j(\neq\theta_i)=0$ (see Fig. 1). The additional discontinuity behaviors are not allowable and are remedied by multiplying $\sin^2(\theta_j/2)$ to $\hat{w}_{n,A}(\lambda_n, r_i, \theta_i)$ and $\hat{w}_{n,S}(\lambda_n, r_i, \theta_i)$ in Eqs. (6e) and (6f). Function $\sin^2(\theta_j/2)$ not only restricts the discontinuities of $\tilde{w}_{n,A}$ and the first derivatives of $\tilde{w}_{n,S}$ across the crack only, but also retains the symmetry features of $\hat{w}_{n,A}$ and $\hat{w}_{n,S}$. Because the first differential of $\sin^2(\theta_j/2)$ with respect to x or y is singular at $r_j=0$, r_j^{κ} with $\kappa \geq 1.5$ is multiplied to $\sin^2(\theta_j/2)$ to avoid the unsuitable singularities. When κ is set equal to 1.5, $\tilde{w}_{n,A}(\lambda_n, r_i, \theta_i, r_j, \theta_j)$ and $\tilde{w}_{n,S}(\lambda_n, r_i, \theta_i, r_j, \theta_j)$ not only appropriately describe the behaviors of stress singularities at the neighborhood of $r_i \to 0$ but also match the stress singularity orders at $r_j=0$.

For simplicity, N_1, N_2, N_3, and N_4 in Eq. (5) are all set equal to N in the following computations. Substituting Eqs. (3)–(6) into Eqs. (1) and (2) and minimizing the functional Π with respect to undetermined coefficients A_{ij}, C_n, D_n, E_n, and F_n yields $IJ+4N$ linear algebraic equations for those coefficients to be determined, and results in an eigenvalue problem with the eigenvalues related to the natural frequencies of plate. To solve the eigenvalue problem accurately, variables with 128-bit precision (with approximately 34 decimal digit accuracy) were used in the developed computer programs.

Notably, subroutine "DTWODQ" in IMSL was adapted to evaluate the integrals of functions involved in establishing the matrixes in the eigenvalue problem. This subroutine integrates a function by means of a globally adaptive scheme based on Gauss–Kronrod rules [22]. When $\tilde{w}_{n,A}(\lambda_n, r_i, \theta_i, r_j, \theta_j)$, $\tilde{w}_{n,S}(\lambda_n, r_i, \theta_i, r_j, \theta_j)$ and their derivatives are involved in the integration, the whole integration domain is divided into six sub-domains as shown in Fig. 2, and the crack is not inside any one of the sub-domains.

3. Convergence studies

Since cracked square plates with simple support boundary conditions were often studied in the published literature, convergence studies were carried out for such plates with different

crack lengths to verify the correctness of the solutions and demonstrate the effects of W_c on the solutions. In Eq. (5) l, m, p, and q are set equal one to satisfy the geometric boundary conditions (zero transverse displacement) along simply supported edges. Numerical results are presented for the first five nondimensional frequency parameters $\omega a^2\sqrt{\rho h/D}$, which are commonly used in the plate vibration literature, of plates having centrally located cracks ($x_0/a=0.5$ and $y_0/b=0.5$) with different crack lengths ($d/a=0.2$, 0.5, and 0.8) and inclination angles ($\alpha=0^\circ$ and 45°). Poisson's ratio equal to 0.3 is used for all the results shown here.

Shown in Tables 1–3 are the convergence studies of nondimensional frequency parameters for horizontally cracked plates with length $d/a=0.2$, 0.5, and 0.8, respectively. The middle point of the crack coincides with the center of plate. In the first column of these tables parenthesized S and A denote symmetric and anti-symmetric mode shapes, respectively, with respect to the line of crack. The present solutions did not take advantage of the symmetry of the problem. That is, the solutions for symmetric and anti-symmetric modes were not separately considered. The published results by Stahl and Keer [10], Liew et al. [7], and Su et al. [17] are also listed for comparison. It should be noted that although Stahl and Keer [10] used a very accurate Fredholm integration approach, they admitted that the fourth significant figure of their results for the higher modes may not be accurate because of the numerical techniques used in determining the natural frequencies. Liew et al. [7] decomposed the plate under consideration into three sub-domains and used 19×9 terms of orthogonal polynomials for each sub-domain to construct the solutions for symmetric and anti-symmetric modes, respectively. As mentioned in Section 1, the solutions of Liew et al. [7] are not guaranteed to be the upper bounds on exact natural frequencies. Su et al. [17] used a finite element approach without mentioning the element size or number.

The numerical results for a plate with a short horizontal crack ($d/a=0.2$) in Table 1 are shown as 5×5, 6×6,…, 10×10 terms of orthogonal polynomials are retained in Eq. (4) in conjunction with 0, 20, 40, and 60 modified corner functions in Eq. (5). The results obtained by using polynomials and no modified corner functions ($N=0$ in W_c) converge to the exact results for a simply supported intact square plate[2]; that is, integer multiplies of π^2. This observation is expected because the solutions from the Ritz method with polynomial admissible functions (Eq. (4)) alone cannot realize the existence of a crack. Adding a small number of modified corner functions into the admissible functions significantly improves numerical solutions. The numerical solutions converge very well by simultaneously increasing the number of polynomial terms and modified corner functions. Using $I=J=9$ and $N=10$ (totally 121 terms) in the admissible functions leads to at least three significant figure convergence, and the convergent results show excellent agreement with those of Stahl and Keer [10], while the results of Su et al. [17] and Liew et al.[7] agree well with those of Stahl and Keer [10]. The fifth nondimensional frequency obtained by Liew et al. [7] is significantly larger than the present one and is clearly less accurate because the present upper bound solutions are shown to have converged to four significant figures.

Convergence studies for larger horizontal cracks (i.e., $d/a=0.5$ and 0.8) are shown in Tables 2 and 3. The numerical results are shown as 4×4, 5×5,…, 9×9 terms of orthogonal polynomials are used in Eq. (4) in conjunction with 0, 20, 40, 60, and 80 modified corner functions in Eq. (5). Again, using larger numbers of modified corner functions and polynomial functions yields better convergent solutions. Convergence to at least three significant figure has been achieved with $I=J=9$ and $N=15$ (totally 141 terms) in the admissible functions. The convergent results show better agreement with those of Stahl and Keer [10] than the results of Liew et al. [7], and Su et al. [17] do. Notably,

Table 1
Convergence of frequency parameters $\omega a^2\sqrt{\rho h/D}$ for a simply supported square plate with a horizontal center crack ($x_0/a=y_0/b=0.5$, $d/a=0.2$, $\alpha=0^\circ$).

Mode no.	N_1, N_2, N_3, N_4 *for* W_c in Eq. (5)	Orthogonal polynomials ($I\times J$)						Published results
		5×5	6×6	7×7	8×8	9×9	10×10	
1(S)	0	19.74	19.74	19.74	19.74	19.74	19.74	
	5	19.46	19.46	19.39	19.39	19.35	19.35	[19.3]
	10	19.39	19.39	19.34	19.34	19.33	19.33	(19.38)
	15	19.37	19.37	19.33	19.33	19.33	19.32	{19.3}
2(A)	0	49.49	49.35	49.35	49.35	49.35	49.35	
	5	49.22	49.20	49.20	49.19	49.19	49.19	[49.17]
	10	49.20	49.19	49.19	49.19	49.19	49.18	(49.16)
	15	49.19	49.19	49.19	49.19	49.19	49.18	{49.15}
3(S)	0	49.49	49.35	49.35	49.35	49.35	49.35	
	5	49.33	49.33	49.33	49.33	49.33	49.32	[49.33]
	10	49.33	49.33	49.33	49.33	49.32	49.32	(49.31)
	15	49.33	49.33	49.33	49.32	49.32	49.32	{49.29}
4(A)	0	79.17	78.96	78.96	78.96	78.96	78.96	
	5	78.98	78.96	78.96	78.95	78.95	78.95	[78.96]
	10	78.96	78.95	78.95	78.95	78.95	78.95	(78.81)
	15	78.95	78.95	78.95	78.95	78.95	78.95	{78.68}
5(S)	0	100.1	100.1	98.72	98.72	98.70	98.70	
	5	95.85	95.85	94.85	94.85	94.38	94.38	[93.96]
	10	94.95	94.95	94.29	94.29	94.13	94.13	(94.69)
	15	94.70	94.70	94.21	94.21	94.11	94.11	{94.24}

Note: [ ]: results from Stahl and Keer [10].
( ): results from Liew et al. [7].
{ }: results from Su et al. [17].

Table 2
Convergence of frequency parameters $\omega a^2\sqrt{\rho h/D}$ for a simply supported square plate with a horizontal center crack ($x_0/a=y_0/b=0.5$, $d/a=0.5$, $\alpha=0^\circ$).

Mode no.	N_1, N_2, N_3, N_4 *for* W_c in Eq. (5)	Orthogonal polynomials ($I\times J$)						Published results
		4×4	5×5	6×6	7×7	8×8	9×9	
1(S)	0	19.74	19.74	19.74	19.74	19.74	19.74	
	5	17.81	17.75	17.75	17.73	17.72	17.72	[17.7]
	10	17.80	17.73	17.73	17.72	17.72	17.72	(17.85)
	15	17.76	17.73	17.73	17.72	17.72	17.72	{17.7}
	20	17.75	17.72	17.72	17.72	17.72	17.72	
2(A)	0	49.49	49.49	49.35	49.35	49.35	49.35	
	5	43.48	43.28	43.20	43.11	43.08	43.07	[43.03]
	10	43.22	43.12	43.11	43.08	43.07	43.06	(42.82)
	15	43.14	43.10	43.07	43.07	43.06	43.06	{43.25}
	20	43.13	43.09	43.07	43.06	43.06	43.06	
3(S)	0	49.49	49.49	49.35	49.35	49.35	49.35	
	5	48.85	48.70	48.69	48.69	48.69	48.69	[48.70]
	10	48.70	48.69	48.69	48.69	48.69	48.69	(48.72)
	15	48.70	48.69	48.69	48.69	48.69	48.69	{48.72}
	20	48.69	48.69	48.69	48.69	48.69	48.69	
4(A)	0	79.17	79.17	78.96	78.96	78.96	78.96	
	5	77.92	77.92	77.76	77.76	77.74	77.74	[77.73]
	10	77.73	77.73	77.73	77.73	77.72	77.72	(77.44)
	15	77.73	77.73	77.72	77.72	77.72	77.72	{77.54}
	20	77.73	77.73	77.72	77.72	77.72	77.72	
5(S)	0	139.6	100.1	100.1	98.72	98.72	98.70	
	5	84.98	82.90	82.90	82.36	82.36	82.22	[82.15]
	10	84.32	82.44	82.44	82.23	82.23	82.19	(83.01)
	15	83.12	82.30	82.30	82.22	82.22	82.18	{82.39}
	20	82.80	82.28	82.28	82.20	82.20	82.17	

Note: [ ]: results from Stahl and Keer [10].
( ): results from Liew et al. [7].
{ }: results from Su et al. [17].

Table 3
Convergence of frequency parameters $\omega a^2\sqrt{\rho h/D}$ for a simply supported square plate with a horizontal center crack ($x_0/a=y_0/b=0.5$, $d/a=0.8$, $\alpha=0^\circ$).

Mode no.	N_1, N_2, N_3, N_4 for W_c in Eq. (5)	Orthogonal polynomials ($I\times J$)						Published results
		4×4	5×5	6×6	7×7	$8\times\times8$	9×9	
1(S)	0	19.74	19.74	19.74	19.74	19.74	19.74	
	5	16.45	16.42	16.42	16.42	16.42	16.42	[16.4]
	10	16.43	16.41	16.41	16.41	16.41	16.41	(16.47)
	15	16.43	16.41	16.41	16.41	16.41	16.41	{16.4}
	20	16.42	16.41	16.41	16.41	16.41	16.41	
2(A)	0	49.49	49.49	49.35	49.35	49.35	49.35	
	5	29.40	28.04	27.99	27.98	27.97	27.97	[27.77]
	10	28.03	27.97	27.84	27.82	27.80	27.80	(27.43)
	15	28.02	27.85	27.81	27.80	27.79	27.77	{28.01}
	20	28.01	27.83	27.81	27.79	27.78	27.77	
3(S)	0	49.49	49.49	49.35	49.35	49.35	49.35	
	5	47.41	47.25	47.23	47.23	47.23	47.22	[47.26]
	10	47.23	47.22	47.22	47.21	47.21	47.21	(47.27)
	15	47.23	47.21	47.21	47.21	47.21	47.21	{47.30}
	20	47.22	47.21	47.21	47.21	47.21	47.21	
4(A)	0	79.17	79.17	78.96	78.96	78.96	78.96	
	5	66.53	66.53	66.50	66.50	66.49	66.49	[65.73]
	10	65.94	65.94	65.90	65.90	65.89	65.89	(65.19)
	15	65.92	65.92	65.78	65.78	65.77	65.77	{65.97}
	20	65.88	65.88	65.78	65.78	65.76	65.76	
5(S)	0	139.6	100.1	100.1	98.72	98.72	98.70	
	5	77.83	77.16	77.16	76.47	76.47	76.41	[76.37]
	10	77.12	76.49	76.49	76.39	76.39	76.37	(76.60)
	15	76.71	76.43	76.43	76.38	76.38	76.37	{76.39}
	20	76.64	76.40	76.40	76.37	76.37	76.37	

Note [ ]: results from Stahl and Keer [10].
( ): results from Liew et al. [7].
{ }: results from Su et al. [17].

Table 4
Convergence of frequency parameters $\omega a^2\sqrt{\rho h/D}$ for the same case as Table 1, but using $\kappa=\overline{\kappa}=2.5$ in Eq. (6a–h).

Mode no.	N_1, N_2, N_3, N_4 for W_c in Eq. (5)	Orthogonal polynomials ($I\times J$)						Published results
		5×5	6×6	7×7	8×8	9×9	11×11	
1(S)	0	19.74	19.74	19.74	19.74	19.74	19.74	
	5	19.54	19.54	19.46	19.46	19.45	19.41	[19.3]
	10	19.46	19.46	19.45	19.45	19.40	19.35	(19.38)
	15	19.45	19.45	19.42	19.42	19.36	19.34	{19.3}
2(A)	0	49.49	49.35	49.35	49.35	49.35	49.35	
	5	49.26	49.23	49.21	49.20	49.20	49.19	[49.17]
	10	49.22	49.20	49.20	49.20	49.19	49.19	(49.16)
	15	49.21	49.20	49.20	49.19	49.19	49.19	{49.15}
3(S)	0	49.49	49.35	49.35	49.35	49.35	49.35	
	5	49.34	49.33	49.33	49.33	49.33	49.33	[49.33]
	10	49.34	49.33	49.33	49.33	49.33	49.32	(49.31)
	15	49.34	49.33	49.33	49.33	49.33	49.32	{49.29}
4(A)	0	79.17	78.96	78.96	78.96	78.96	78.96	
	5	78.96	78.95	78.95	78.95	78.95	78.95	[78.96]
	10	78.95	78.95	78.95	78.95	78.95	78.95	(78.81)
	15	78.95	78.95	78.95	78.95	78.95	78.95	{78.68}
5(S)	0	100.1	100.1	98.72	98.72	98.70	98.70	
	5	96.52	96.52	95.59	95.59	95.53	95.03	[93.96]
	10	95.62	95.62	95.44	95.44	94.95	94.43	(94.69)
	15	95.53	95.53	95.15	95.15	94.51	94.32	{94.24}

Note: [ ]: results from Stahl and Keer [10].
( ): results from Liew et al. [7].
{ }: results from Su et al. [17].

the results of Liew et al. [7] were obtained using 513 admissible functions, which are much more than that used for the present results. In terms of the first three significant figures, the second and fourth frequencies, in Tables 2 and 3, obtained by Liew et al. are less than those of Stahl and Keer, another indication that the solutions of Liew et al. are not guaranteed to be upper bounds on the exact frequencies.

It should be specially mentioned that the present results were obtained by using $\kappa=\overline{\kappa}=1.5$ in Eq. (6). To show the effects of different values of κ and $\overline{\kappa}$ on the convergence of solutions, similar to the presentation in Tables 1 and 3, Tables 4 and 5 illustrate the corresponding convergence studies by using $\kappa=\overline{\kappa}=2.5$ in Eq. (6). Comparing Tables 4 and 5 with Tables 1 and 3, respectively, one finds that the convergence rates of the solutions are slightly changed when changing $\kappa=\overline{\kappa}=1.5$–$2.5$.

To investigate the effects of crack inclination and boundary conditions of the plate on the convergence of the present solutions, Table 6 summarizes the convergence studies of nondimensional frequency parameters for a simply supported square plate with an inclined crack ($\alpha=45^\circ$) having length $d/a=0.5$, while Table 7 shows the convergence study for a completely free square plate with a horizontal crack having length $d/a=0.5$. The middle point of the crack coincides with the center of plate. Notably, there are three rigid body modes for a complete free plate, having zero frequencies, which are not shown in Table 7. Comparing these data with those in Table 2, one finds that the convergence rates of frequencies with increased number of modified corner functions in the admissible functions are different for the results in these three tables. However, using $I=J=9$ and $N=15$ (totally 141 terms) in the admissible functions still gives at least three

Table 5
Convergence of frequency parameters $\omega a^2\sqrt{\rho h/D}$ for the same case as Table 3, but using $\kappa=\overline{\kappa}=2.5$ in Eq. (6a–h).

Mode no.	N_1, N_2, N_3, N_4 for W_c in Eq. (5)	Orthogonal polynomials ($I\times J$)						Published results
		4×4	5×5	6×6	7×7	8×8	9×9	
1(S)	0	19.74	19.74	19.74	19.74	19.74	19.74	
	5	16.69	16.44	16.44	16.42	16.42	16.41	[16.4]
	10	16.45	16.42	16.42	16.41	16.41	16.41	(16.47)
	15	16.43	16.41	16.41	16.41	16.41	16.41	{16.4}
	20	16.42	16.41	16.41	16.41	16.41	16.41	
2(A)	0	49.49	49.49	49.35	49.35	49.35	49.35	
	5	28.38	28.05	28.04	28.01	27.99	27.98	[27.77]
	10	27.92	27.89	27.83	27.81	27.81	27.80	(27.43)
	15	27.87	27.81	27.80	27.80	27.78	27.77	{28.01}
	20	27.86	27.80	27.79	27.79	27.77	27.77	
3(S)	0	49.49	49.49	49.35	49.35	49.35	49.35	
	5	47.39	47.25	47.22	47.22	47.21	47.21	[47.26]
	10	47.23	47.21	47.21	47.21	47.21	47.21	(47.27)
	15	47.22	47.21	47.21	47.21	47.21	47.21	{47.30}
	20	47.21	47.21	47.21	47.21	47.21	47.21	
4(A)	0	79.17	79.17	78.96	78.96	78.96	78.96	
	5	66.07	66.07	65.97	65.97	65.90	65.90	[65.73]
	10	65.90	65.90	65.84	65.84	65.77	65.77	(65.19)
	15	65.85	65.85	65.78	65.78	65.76	65.76	{65.97}
	20	65.84	65.84	65.76	65.76	65.76	65.76	
5(S)	0	139.6	100.1	100.1	98.72	98.72	98.70	
	5	79.40	76.77	76.77	76.46	76.46	76.38	[76.37]
	10	77.68	76.51	76.51	76.38	76.38	76.37	(76.60)
	15	76.78	76.39	76.39	76.38	76.38	76.37	{76.39}
	20	76.63	76.38	76.38	76.37	76.37	76.37	

Note: [ ]: results from Stahl and Keer [10].
( ): results from Liew et al. [7].
{ }: results from Su et al. [17].

Table 6
Convergence of frequency parameters $\omega a^2\sqrt{\rho h/D}$ for a simply supported square plate with an inclined center crack ($x0/a=y_0/b=0.5$, $d/a=0.5$, $\alpha=45^\circ$).

Mode no.	N_1, N_2, N_3, N_4 *for* W_c in Eq. (5)	Orthogonal polynomials ($I\times J$)					
		4×4	5×5	6×6	7×7	8×8	9×9
1	0	19.74	19.74	19.74	19.74	19.74	19.74
	5	17.60	17.57	17.54	17.54	17.53	17.53
	10	17.57	17.55	17.54	17.54	17.53	17.53
	15	17.57	17.54	17.54	17.53	17.53	17.53
	20	17.56	17.54	17.53	17.53	17.53	17.53
2	0	49.49	49.49	49.35	49.35	49.35	49.35
	5	43.46	43.07	42.92	42.91	42.87	42.86
	10	42.97	42.93	42.88	42.87	42.86	42.85
	15	42.94	42.88	42.86	42.86	42.85	42.85
	20	42.92	42.88	42.86	42.85	42.85	42.85
3	0	49.49	49.49	49.35	49.35	49.35	49.35
	5	48.43	48.43	48.35	48.35	48.34	48.34
	10	48.37	48.37	48.33	48.33	48.33	48.33
	15	48.37	48.36	48.33	48.33	48.33	48.33
	20	48.36	48.36	48.33	48.33	48.33	48.33
4	0	79.17	79.17	78.96	78.96	78.96	78.96
	5	74.43	73.91	73.63	73.58	73.57	73.55
	10	73.92	73.67	73.60	73.57	73.56	73.55
	15	73.89	73.59	73.58	73.56	73.56	73.55
	20	73.87	73.59	73.57	73.56	73.56	73.55
5	0	139.6	100.1	100.1	98.72	98.72	98.70
	5	90.93	90.30	90.20	90.01	90.00	89.96
	10	90.72	90.03	90.03	89.97	89.96	89.95
	15	90.64	90.01	89.99	89.96	89.96	89.95
	20	90.62	89.00	89.98	89.96	89.95	89.95

Table 7
Convergence of frequency parameters $\omega a^2\sqrt{\rho h/D}$ for a completely free square plate with a horizontal center crack ($x_0/a=y_0/b=0.5$, $d/a=0.5$, $\alpha=0^\circ$).

Mode no.	N_1, N_2, N_3, N_4 *for* W_c in Eq. (5)	Orthogonal polynomials ($I\times J$)					
		4×4	5×5	6×6	7×7	8×8	9×9
1(A)	0	13.66	13.66	13.47	13.47	13.47	13.47
	5	13.50	13.50	13.47	13.47	13.47	13.47
	10	13.47	13.47	13.47	13.47	13.47	13.47
	15	13.47	13.47	13.47	13.47	13.47	13.47
	20	13.47	13.47	13.47	13.47	13.47	13.47
2(S)	0	22.45	19.73	19.73	19.60	19.60	19.60
	5	18.34	17.88	17.88	17.64	17.64	17.60
	10	17.99	17.67	17.67	17.61	17.61	17.59
	15	17.90	17.65	17.65	17.61	17.61	17.59
	20	17.79	17.63	17.63	17.60	17.60	17.58
3(S)	0	30.59	24.54	24.54	24.27	24.27	24.27
	5	22.48	22.15	22.15	22.12	22.12	22.11
	10	22.35	22.13	22.13	22.11	22.11	22.10
	15	22.24	22.13	22.13	22.11	22.11	22.10
	20	22.19	22.12	22.12	22.11	22.11	22.10
4(A)	0	39.23	35.61	35.29	34.81	34.80	34.80
	5	34.50	34.35	33.81	33.68	33.67	33.66
	10	33.75	33.71	33.67	33.66	33.65	33.65
	15	33.72	33.68	33.65	33.65	33.65	33.65
	20	33.71	33.67	33.65	33.65	33.65	33.64
5(S)	0	39.23	35.61	35.29	34.81	34.80	34.80
	5	35.08	34.88	34.55	34.40	34.40	34.40
	10	34.50	34.43	34.40	34.39	34.39	34.39
	15	34.44	34.40	34.39	34.39	34.39	34.39
	20	34.42	34.40	34.39	34.39	34.39	34.39

significant figure convergence for the first five nonzero frequencies in each case.

4. Frequencies and mode shapes

Based on the convergence studies given in the previous section, $I=J=9$ and $N=10$ (totally 121 terms) and $I=J=9$ and $N=15$ (totally 141 terms) in the admissible functions were employed to determine the first five nonzero frequencies and corresponding mode shapes of square cracked plates having crack length $d/a\leq0.3$ and $d/a\geq0.4$, respectively. Tables 8 and 9, respectively, list the nondimensional frequency parameters for simply supported and completely free square plates having internal cracks with various lengths ($d/a=0.1, 0.2,\ldots,0.6$), different inclination angles ($\alpha=0^\circ$, 15°, 30°, and 45°), and different locations ((x_0/a, y_0/b)=(0.5, 0.5) and (0.5, 0.75)). All frequency results are guaranteed upper bounds to the exact values and are exact to at least three significant figures. This is the most comprehensive and accurate set of frequencies to date for rectangular plates with internal cracks or slits. It is also the first published vibration data for cracks, which are inclined ($\alpha\neq0^\circ$) and for completely free plates with internal cracks.

Results of Stahl and Keer [10] for simply supported cracked plates are also given in Table 8. Agreement with at least three significant figures is found between the present results and results of Stahl and Keer, who achieved their excellent results in 1972 with much less computer capability.

The first five nondimensional frequency parameters for a simply supported square plate with no cracks are 19.74, 49.35, 49.35, 78.96, and 98.70 (see Table 1), and they are 13.47, 19.60, 24.27, 34.80, and 34.80 (see Table 7) for a completely free intact plate. The differences in frequencies between intact plates and cracked plates with small crack length ($d/a=0.1$) are much less than 1%, regardless of the orientation and location of crack.

It is clear that increasing crack length leads to decreasing frequencies because of the decrease in stiffness in a plate, with no significant change in its mass. This is clearly seen for most of the vibration modes in Tables 8 and 9. Nevertheless, for completely free plates (Table 9) the first nonzero frequencies with horizontal cracks and the fifth nonzero frequencies with inclined cracks ($\alpha=30^\circ$ and 45°) are not sensitive to the crack length. The changes in frequency for such modes are less than 0.3% when $d/a=0$ changes to $d/a=0.6$.

Some clear effects of the orientation of crack on the natural frequencies are observed from Tables 8 and 9. In the cases of simply supported plates, increasing the inclined angle of crack ($\alpha=0^\circ$ changes to 45°) yields the decrease in first four frequencies. Different trends are found for completely free plates, and increase in α causes the decrease in first and third frequencies but the increase in second, fourth, and fifth frequencies.

For plates with center cracks ((x_0/a, y_0/b)=(0.5, 0.5)) on one of their symmetry axes, the vibration mode shapes are still either symmetric or anti-symmetric to the axes. This is observed in the nodal patterns (lines of zero vibration displacement) shown in Figs. 3 and 4 when $\alpha=0^\circ$ or 45°. When $\alpha=0^\circ$ and $d/a=0.2$ (a small horizontal crack), the small crack only cause the fifth mode shape significantly different from that for an intact plate with simply support conditions; and similar observation is found for the second modes for completely free plates. As the crack is getting large ($d/a=0.6$), more significant changes are revealed for such modes as well as for the third and fourth modes for completely free cracked plates. Adding an inclined crack with $\alpha=45^\circ$ to an intact plate leads to substantial changes of modal shapes in the fourth and fifth modes with simple support boundary conditions and in the first mode for completely free boundary conditions.

When a horizontal crack is not on the symmetry axis of the plate but its middle point is, the mode shapes of the cracked plate are either symmetric or anti-symmetric to the symmetry axis

Table 8
Frequency parameters $\omega a^2\sqrt{\rho h/D}$ for simply supported square plates with internal cracks at various locations and with different orientation and lengths.

α (deg.)	$(x_0/a, y_0/b)$	d/a	Mode				
			1	2	3	4	5
0	(0.5, 0.5)	0.1	19.66	49.34	49.35	78.96	97.79
		0.2	19.33 [19.3]	49.19 [49.17]	49.32 [49.33]	78.95 [78.96]	94.13 [93.96]
		0.3	18.85	48.50	49.24	78.89	89.73
		0.4	18.29 [18.2]	46.65 [46.62]	49.03 [49.03]	78.61 [78.60]	85.56 [85.51]
		0.5	17.72 [17.7]	43.06 [43.03]	48.69 [48.70]	77.72 [77.73]	82.18 [82.15]
		0.6	17.19 [17.1]	37.99 [37.98]	48.22 [48.22]	75.59 [75.58]	79.60 [79.59]
0	(0.5, 0.75)	0.1	19.69	48.95	49.35	78.95	98.17
		0.2	19.51	47.60	49.34	78.88	96.29
		0.3	19.22	45.77	49.29	78.57	93.04
		0.4	18.81	43.81	49.15	77.86	85.95
		0.5	18.30	41.92	48.89	73.05	76.69
		0.6	17.73	40.08	48.44	60.50	75.15
15	(0.5, 0.5)	0.1	19.65	49.34	49.35	78.93	97.78
		0.2	19.33	49.18	49.32	78.79	94.39
		0.3	18.85	48.48	49.23	78.43	90.43
		0.4	18.27	46.60	49.00	77.59	87.04
		0.5	17.67	43.00	48.60	76.10	84.57
		0.6	17.10	37.96	48.06	74.03	82.19
30	(0.5, 0.5)	0.1	19.66	49.34	49.35	78.88	97.84
		0.2	19.32	49.17	49.32	78.49	94.86
		0.3	18.83	48.44	49.20	77.63	91.71
		0.4	18.23	46.52	48.92	76.14	89.46
		0.5	17.58	42.91	48.43	74.25	88.14
		0.6	16.93	37.87	47.70	72.29	84.71
45	(0.5, 0.5)	0.1	19.66	49.34	49.35	78.85	97.89
		0.2	19.32	49.17	49.32	78.35	95.12
		0.3	18.82	48.41	49.19	77.27	92.31
		0.4	18.21	46.48	48.89	75.56	90.57
		0.5	17.53	42.85	48.33	73.55	89.95
		0.6	16.84	37.85	47.51	71.60	84.58

Note: [ ]: results of Stahl and Keer [10].

Table 9
Frequency parameters $\omega a^2\sqrt{\rho h/D}$ for completely free square plates with internal cracks at various locations and with different orientation and lengths.

α (deg.)	$(x_0/a, y_0/b)$	d/a	Mode				
			1	2	3	4	5
0	(0.5, 0.5)	0.1	13.47	19.57	24.18	34.80	34.80
		0.2	13.47	19.40	23.73	34.77	34.79
		0.3	13.47	19.07	23.14	34.66	34.75
		0.4	13.47	18.50	22.55	34.34	34.63
		0.5	13.47	17.59	22.10	33.65	34.39
		0.6	13.46	16.41	21.82	32.26	33.98
0	(0.5, 0.75)	0.1	13.47	19.59	24.23	34.79	34.80
		0.2	13.47	19.55	24.06	34.75	34.80
		0.3	13.47	19.46	23.78	34.64	34.79
		0.4	13.47	19.28	23.39	34.39	34.76
		0.5	13.46	18.96	22.91	33.91	34.70
		0.6	13.45	18.36	22.43	33.02	34.56
15	(0.5, 0.5)	0.1	13.46	19.58	24.18	34.80	34.80
		0.2	13.44	19.45	23.73	34.78	34.79
		0.3	13.41	19.20	23.13	34.68	34.76
		0.4	13.34	18.76	22.50	34.41	34.69
		0.5	13.24	18.08	22.01	33.81	34.54
		0.6	13.06	17.21	21.69	32.55	34.28
30	(0.5, 0.5)	0.1	13.46	19.59	24.17	34.80	34.80
		0.2	13.40	19.55	23.73	34.79	34.80
		0.3	13.29	19.47	23.09	34.74	34.79
		0.4	13.13	19.31	22.39	34.59	34.78
		0.5	12.89	19.05	21.75	34.21	34.77
		0.6	12.54	18.66	21.29	33.31	34.74
45	(0.5, 0.5)	0.1	13.46	19.60	24.19	34.80	34.80
		0.2	13.38	19.60	23.73	34.80	34.80
		0.3	13.24	19.60	23.07	34.78	34.80
		0.4	13.03	19.59	22.31	34.71	34.80
		0.5	12.74	19.58	21.55	34.50	34.79
		0.6	12.35	19.56	20.86	33.89	34.78

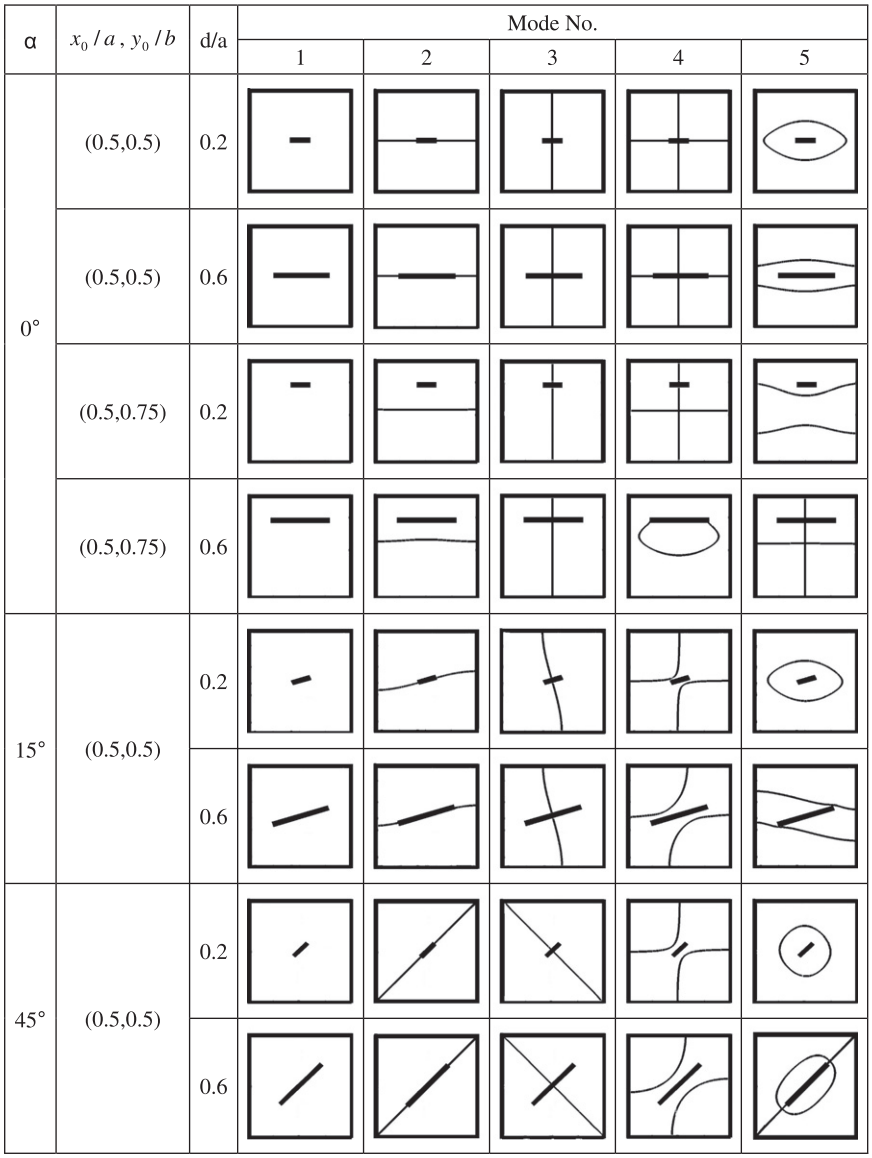

Fig. 3. Nodal patterns for a simply supported square plate with an internal crack.

perpendicular to the crack. This is found in Figs. 3 and 4 when $\alpha=0^\circ$ and $(x_0/a,\ y_0/b)=(0.5,\ 0.75)$. The existence of the crack causes significant changes in the mode shapes of the symmetric modes from those for an intact plate.

When a crack completely destroys the symmetry of plate, the crack causes considerable changes in all mode shapes from those for an intact plate, which is seen in Figs. 3 and 4 when $\alpha=15^o$. When the crack length becomes larger, the changes in mode shapes become more significant.

5. Concluding remarks

This paper has proposed a new set of admissible functions for plates with internal cracks for the Ritz method based on the classical plate theory. The proposed set of admissible functions is capable of describing the stress singularity behaviors around the crack tips and showing discontinuities of the transverse displacement and slopes across the crack. The main superiority of the present solutions over the existing solutions based on the Ritz method is that the present solutions guarantees to provide upper bounds to the exact solutions, which is very important feature for a good numerical solution. Additionally, the present solutions using a less number of admissible functions are at least as accurate as those previously published.

The proposed solutions have been validated through comprehensive convergence studies for simply supported plates having cracks with various lengths. The convergent solutions show excellent agreement with those obtained by Stahl and Keer [10] accurately solving homogeneous Fredholm integral equations. The proposed solutions have been further applied to obtain the accurate frequencies and nodal patters for simply supported and completely free square plates having internal cracks at different locations ($(x_0/a,\ y_0/b)=(0.5,\ 0.5)$ and $(0.5,\ 0.75)$), with various lengths ($d/a=0.1$–0.6) and orientations ($\alpha=0^\circ$, 15°, 30°, and 45°). The results are novel, and are the first published vibration data for cracks which are inclined ($\alpha\neq 0^\circ$) and for completely free plates with internal cracks.

Although only rectangular plates with straight internal cracks have been investigated here, the present solutions are easy to extend to consider plates with other shapes (i.e., circular or skew trapezoidal plates) through proper transformations of coordinates. The present approach can also be extended to consider plates with multiple cracks, and each crack needs a set of the proposed admissible functions. Furthermore, there are lots of possible

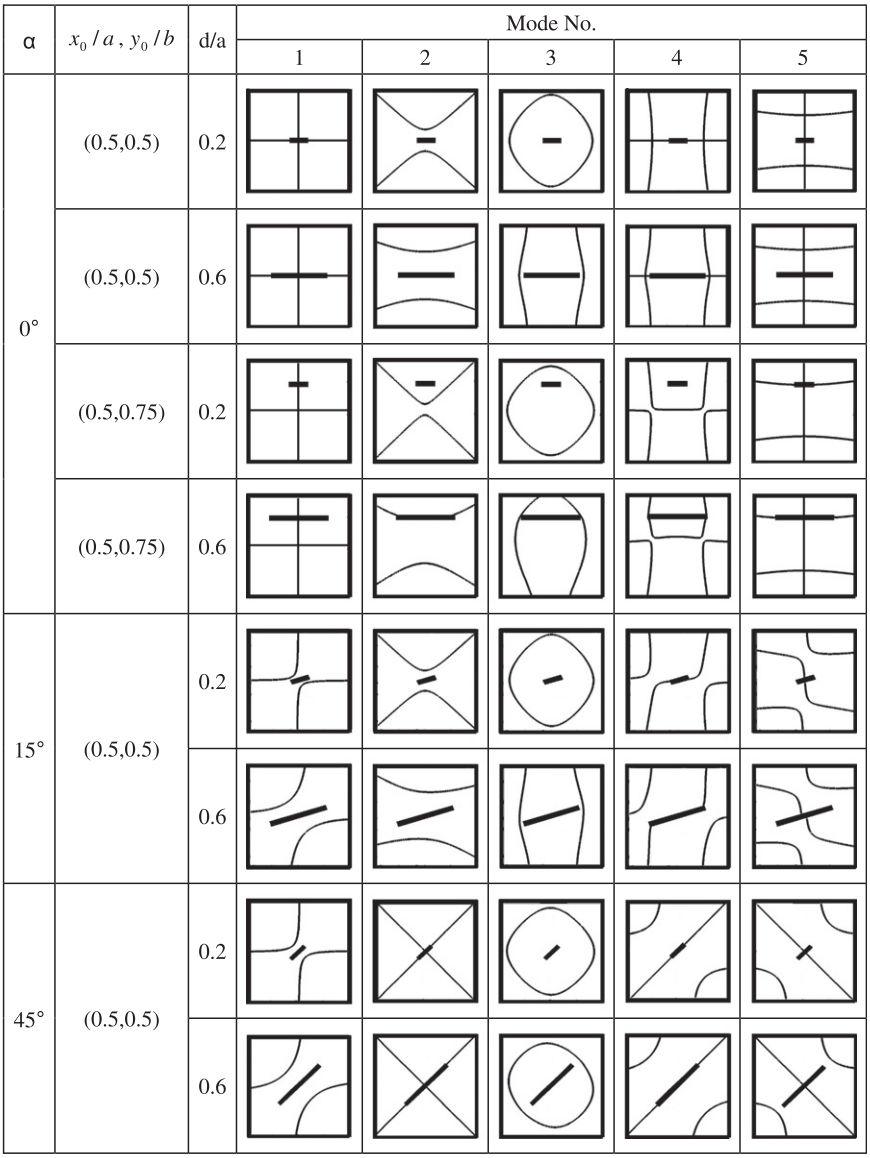

Fig. 4. Nodal patterns for a completely free square plate with an internal crack.

extensions of the present work. It will be interesting to explore the possibility of applying similar methodology to determine stress intensity factors of a cracked thin plate because the Ritz method is recognized to be not good in accurately determining stress resultants. The proposed methodology of constructing modified corner functions can be extended to analyze vibrations of thick plates with internal cracks based on the first order or third order shear deformation plate theory or 3D elasticity theory. The proposed set of modified corner functions can be further applied to the element free Galerkin method for accurately solving the static or dynamic problems of plates involving internal cracks. It is believed that only the few terms of the modified corner functions with lower orders in r_1 or r_2 combining with regular polynomial basis functions will be sufficient for solving such problems.

Acknowledgments

The authors would like to thank the National Science Council of the Republic of China, Taiwan, for financially supporting this research under Contract no. NSC 97-2221-Z-009-075-MY3. Much appreciation is extended to National Center for High-performance Computing for granting the supercomputer resources.

References

[1] Ritz W. Über eine neue methode zur lösung gewisser variationsprobleme der mathematischen physik. Journal für Reine und Angewandte Mathematik 1908;135:1–61.
[2] Leissa AW. Vibration of plates. NASA SP-160, US Government Printing Office, 1969. Reprinted by The Acoustical Society of America; 1993.
[3] Leissa AW. Recent research in plate vibrations, 1973–1976: classical theory. The Shock and Vibration Digest 1977;9(10):13–24.
[4] Leissa AW. Plate vibration research, 1976–1980: classical theory. The Shock and Vibration Digest 1981;13(9):11–22.
[5] Leissa AW. Recent studies in plate vibrations: 1981–1985. Part I. Classical theory. The Shock and Vibration Digest 1987;19(2):11–8.
[6] Yuan J, Dickinson SM. The flexural vibration of rectangular plate systems approached by using artificial springs in the Rayleigh–Ritz method. Journal of Sound and Vibration 1992;159(1):39–55.
[7] Liew KM, Hung KC, Lim MK. A solution method for analysis of cracked plates under vibration. Engineering Fracture Mechanics 1994;48(3):393–404.
[8] Khadem SE, Rezaee M. Introduction of modified comparison functions for vibration analysis of a rectangular cracked plate. Journal of Sound and Vibration 2000;236(2):245–58.
[9] Lynn PP, Kumbasar N. Free vibrations of thin rectangular plates having narrow cracks with simply supported edges. Developments in Mechanics.

In: Proceedings of the 10th Midwestern Mechanics Conference, vol. 4, Colorado State University, Fort Collins, Colorado; 1967, p. 911–28.
[10] Stahl B, Keer LM. Vibration and stability of cracked rectangular plates. International Journal of Solids and Structures 1972;8(1):69–91.
[11] Aggarwala BD, Ariel PD. Vibration and bending of a cracked plate. Rozprawy Inzynierskie 1981;29(2):295–310.
[12] Neku K. Free vibration of a simply-supported rectangular plate with a straight through-notch. Bulletin of the Japan Society of Mechanical Engineers 1982;25(199):16–23.
[13] Solecki R. Bending vibration of a simply supported rectangular plate with a crack parallel to one edge. Engineering Fracture Mechanics 1983;18(6): 1111–8.
[14] Hirano Y, Okazaki K. Vibration of cracked rectangular plates. Bulletin of the Japan Society of Mechanical Engineers 1980;23(179):732–40.
[15] Qian GL, Gu SN, Jiang JS. A finite element model of cracked plates and application to vibration problems. Computers and Structures 1991;39(5): 483–7.
[16] Krawczuk M. Natural vibrations of rectangular plates with a through crack. Archive of Applied Mechanics 1993;63(7):491–504.
[17] Su RKL, Leung AYT, Wong SC. Vibration of cracked Kirchhoff's plates. Key Engineering Materials 1998;145–149:167–72.
[18] Ma CC, Huang CH. Experimental and numerical analysis of vibrating cracked plates at resonant frequencies. Experimental Mechanics 2001;41(1):8–18.
[19] Bachene M, Tiberkak R, Rechak S. Vibration analysis of cracked plates using the extended finite element method. Archive of Applied Mechanics 2009;79: 249–62.
[20] Williams ML. Surface stress singularities resulting from various boundary conditions in angular corners of plates under bending. In: Proceedings of the First US National Congress of Applied Mechanics; 1952, p. 325–9.
[21] Bhat RB. Natural frequencies of rectangular plates using characteristic orthogonal polynomials in Rayleigh–Ritz method. Journal of Sound and Vibration 1985;102(4):493–9.
[22] Piessens R, deDoncker-Kapenga E, Uberhuber CW, Kahaner DK. QUADPACK. New York: Springer-Verlag; 1983.